Development of a Streamline Curvature Axial-Flow Compressor Performance Simulator Graphical-User-Interface for Design and Research

Hasani Azamar, Vassilios Pachidis
h.azamaraguirre@cranfield.acuk
Cranfield University
Centre for Propulsion
Cranfield
United Kingdom

Ioannis Templalexis
Hellenic Air Force Academy
Department of Aeronautical Sciences
Athens
Greece

ABSTRACT

The all-time interest to increase turbomachinery efficiencies and pressure ratios has led to the progression of more robust and accurate simulation methods and tools. Even though 3-D CFD analyses are highly detailed and despite the computational power nowadays, they can be costly in terms of time and resources. Conversely, 2-D SLC methods provide acceptable performance and flow field results in short times. Because of economical and practical reasons, SLC still represents the cornerstone for turbomachinery design.

In the present, the knowledge demand from the academia community in the air-breathing engine field has been expanding year after year. Nevertheless, there are very few open-source turbomachinery solvers that can be accessed, where user needs to know at least the basics of the programming language syntax and familiarize with it. For these reasons, a GUI was developed for an existing in-house 2-D SLC axial-flow compressor performance code, called SOCRATES. A GUI in this context supports as a teaching mechanism to explain not only the method itself, but also the compressor aerodynamic behaviour.

The SOCRATES GUI consists in the axial-flow compressor model setup, solution and visualization for geometry and results. This paper outlines the main features of the 2-D SLC GUI, and uses a two-stage fan to show the flow field parameters and compressor/fan map, showing a consistent agreement against measured data.

Keywords: Fan; Compressor; Blade Design; Blade Analysis; Through-flow; Streamline Curvature;

NOMENCLATURE

1-D	One-Dimensional
2-D	Two-Dimensional
3-D	Three-Dimensional
CFD	Computational Fluid Dynamics
DCC	Dynamic Convergence Control
IGV	Inlet Guide Vane
MCA	Multiple-Circular Arc
NACA	National Advisory Committee for Aeronautics
OGV	Outlet Guide Vane
RANS	Reynolds-Averaged Navier-Stokes
REE	Radial Equilibrium Equation
SLC	Streamline Curvature
SOCRATES	Synthesis of Correlations for the Robust Assessment of Turbomachinery Engine Systems

Symbols

w	Mass flow
x	Radial coordinate in Cartesian system
y	Tangential coordinate in Cartesian system
z	Axial coordinate in Cartesian system

1.0 INTRODUCTION

The design of turbomachinery components, such as axial-flow compressors and fans still remains an engineering challenge despite of the technology progress. A number of design and analysis tools have been developed since the 1940s [1] to predict performance, every time increasing robustness and accuracy. One of the first approaches to obtain a one-dimensional (1-D) flow field solution relied on a mean-line or pitch-line method developed by Howell [2], where the flow solution is calculated at the blade mid-span in between adjacent blade rows to obtain the overall component performance.

Wu and Wolfenstein [3] first represented the streamline slope and curvature in the radial equilibrium equation (REE), establishing the cornerstone for two-dimensional (2-D) through-flow calculations. Later, Wright and Kovach [4] considered the streamline curvature (SLC) radius in the radial-axial plane to compute flow calculations. With the further expansion of flow simulation through REE solution, Wright and Novak [5] developed one of the first computational codes. Swan [6] developed a computer program where statistics-based empirical viscous and shock loss models were coupled with the REE. Smith [7] properly defined the REE equation for turbomachinery components and similar works in the United Kingdom were presented by Silvester and Hetherington [8]. Nevertheless, a well-defined SLC method for tubomachinery components was firstly defined and introduced [9,10] by Novak [11].

Quasi three-dimensional (3-D) flow analyses were envisaged by Wu [12], where the concept of the two planes: blade-to-blade (S1) and hub-to-tip (S1), was firstly introduced [1]. With the development of computational power in the 1980s, fully 3-D methods were available. In the present, 3-D computational fluid dynamic (CFD) Reynolds-averaged Navier-Stokes (RANS) numerical simulations play a crucial role in the aerodynamic design for turbomachinery components [13]. Turbomachinery 3-D CFD tools numerically solve the viscosity effects at a small scale, however, it is not an exact science [13]. CFD deviations against real parameters can be due to a) numerical errors related to mesh size and finite difference approximation, b) physics modelling assumptions as in turbulence and transition, c) unknown boundary conditions, d) geometry simplification as in the blade leading edge and tip clearance, and e) steady flow assumption [13]. Additionally, CFD simulations come at high computational costs in terms of solution time and memory, complexity to obtain the required initial and boundary conditions, and lack of flexibility to incorporate or even modify any loss or deviation model [10,14–16]. Under these circumstances, 3-D CFD simulations continue limited to single blade-row models, although there are efforts to conduct multi-stage analyses with the current computational capabilities [17]. Most notable is the fact that in recent years, CFD tools are more widely employed by professionals and young engineers, who despite their expertise, might not realise the CFD drawbacks, representing a potential risk for reliable results procurement.

Alternatively, 2-D through-flow methods provide a quick and fairly acceptable flow solution at low cost in terms of computational run-time and resources [10,15,16,18]. Among the two through-flow techniques known, stream function or matrix method and SLC, the latter is the most widely used [1,19] as it represents the backbone [1,17] for turbomachinery design due to economical and practical reasons [20]. Flow in SLC is assumed to be axisymmetric, compressible, inviscid, and steady. In fact, a fully detailed analysis for an isolated gas-turbine engine component can be obtained through SLC methods. In contrast to CFD, SLC is flexible to incorporate empiricism in the form of loss and deviation models. Besides, SLC numerical simulations require less time to set up the model and the initial and boundary conditions than in 3-D CFD models. Even more, if design optimisation is intended, the 2-D SLC approach avoids the intolerably high 3-D CFD times [20]. Following the progress of 2-D SLC computer programs, several codes have been released over the last 50 years [9,10,19,21–29].

The continuous ambition to increase the compressor efficiencies and pressure ratios has yielded more robust 2-D SLC computational packages. Furthermore, the recent interest of more educators, researchers and students, in the air-breathing engine field has been expanding year after year. Nonetheless, for educational purposes, there are very few open-source tubomachinery solvers available [30]. For instance, turbine codes have been made available, however, user needs to know the commercial package and have a license to run them [31]. Although some compressor and turbine algorithms have been generated as well [32,33], endwall blockage has not been considered. Besides, a comprehensive axisymmetric SLC design system was developed by Turner *et al*. [30], where input files are required to generate the compressor geometry and eventually, obtain the solution.

In this context, a 2-D SLC axial-flow single-stage and multi-stage fan/compressor performance simulator, SOCRATES (Synthesis of Correlations for the Robust Assessment of Turbomachinery Engine Systems), was developed by Pachidis [10], Pachidis *et al*. [14] and Templalexis *et al*. [34], and further improved by Templalexis *et al*. [18] and Templalexis [35]. Templalexis *et al*. [18] explains the SOCRATES structure, where one can find the code-word notation used for the variables and subroutines.

To increase the robustness of SOCRATES, a graphical-user-interface (GUI) was developed for it, motivated by:

- Manual Handling of input and output files opens a window for human errors.
- User needs to familiarize with the input file syntax for compatibility with the code.
- Postprocessing of output file parameters and properties is a time-consuming task that can be automated.
- A GUI for 2-D SLC methods serves as a teaching tool, to understand not only the method itself, but also the concepts and fundamentals for compressor aerodynamic design theory.
- Flexibility in the modification of compressor geometries for blade design.
- Time saving to construct the compressor model and post-process results.
- Feedback from researchers and students that demand more user-friendly tools.

2.0 METHODOLOGY

2.1 2-D SLC Code Structure

The SOCRATES program, coded in FORTRAN 90, follows the 2-D SLC methodology under an iterative technique to re-calculate the streamline position, slope and curvature based on a meridional velocity estimation. Flow field solution is based on the fundamental the Newton's Second Law or conservation of momentum. Because the conservation of momentum already considers the continuity equation, it yields in the Euler equation of motion, which considers the surface traction expressed in terms of the stress field. Due to the inviscid flow assumption, the stress tensor becomes isotropic, resulting in the simplified version of the Navier-Stokes equation for a non-viscous fluid. Within this equation, blade forces are neglected whereas centripetal and Coriolis accelerations are considered. Numerical solution in a cylindrical system, give the full REE to obtain the meridional velocity gradient in the spanwise direction. An initial mesh is generated between the intersection of the assumed initial streamline position, and the inlet and outlet blade rows. REE in set with the mass flow conservation are iteratively solved to satisfy the actual mass flow or outlet static pressure, according to the boundary condition specified. If different, the next loop begins with a new inlet meridional velocity that redefines the streamline radius, and hence, modifying the grid. Streamline radius and shape keeps moving until an agreement is found between the calculated values and specified boundary conditions within a specified error tolerance. Fig. 1 displays a general schematic of the SOCRATES aforementioned processes.

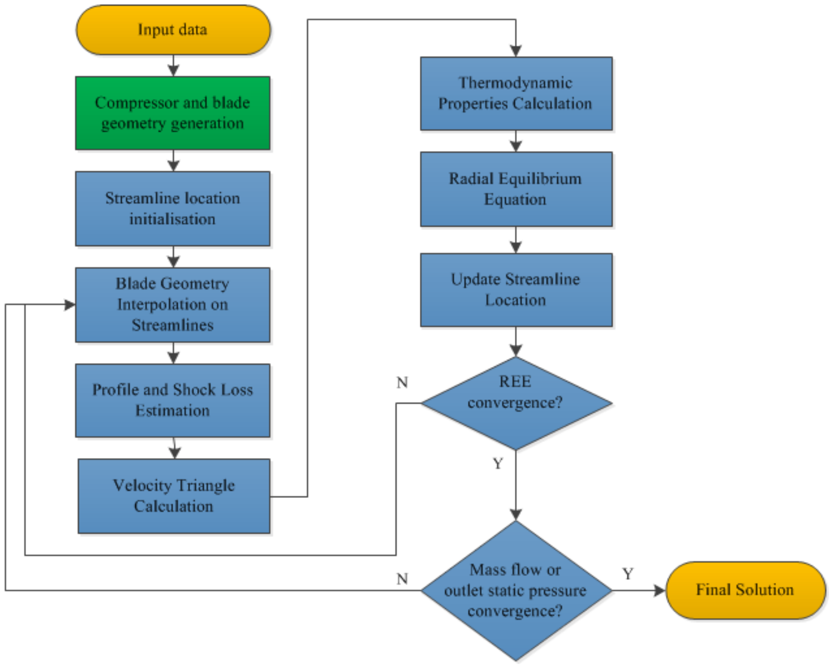

Figure 1 Generic flow chart for the SOCRATES modules.

Due to inviscid flow assumption, empirical correlations are included to compensate for viscosity, deviation and losses. Templalexis *et al.* [18] reported the deviation and loss models included in SOCRATES. Minimum loss incidence angle was calculated with a model from Lieblein [36], while models from Carter [37], Lieblein [38] and Cetin *et al.* [39] were used to calculate deviation angle. Deviation angle at off-design was coded from Creveling and Carmody [21]. Blade row stall prediction was considered from Aungier [40]. Shock Losses were calculated through an empirical correlation that relates a shock loss parameter to the inlet relative Mach number [41].

Besides the flow physics and correlations, the internal iteration algorithms in SOCRATES represent a key feature of the tool. Pachidis *et al.* [42] developed, implemented and tested a dynamic convergence control (DCC) scheme for the solution of the REE in SOCRATES. The new DCC algorithm introduced guarantees convergence, as in every iteration the error tolerance is tightened at a reasonable solution speed. In a separate study by Templalexis [35], the viscous force terms significance in the flow momentum equation and hence, in the REE, was assessed and introduced in SOCRATES. A closer agreement of the SLC flow field against experimental results was found, when the force term is considered. Despite the increase in the REE complexity with the force term addition, more solutions were converged and fewer iterations were required to achieve convergence.

2.2 Graphical-User-Interface

The SOCRATES GUI was coded in Python v. 3.4.3 and it is divided in three main sections: (1) model setup or pre-processing, (2) solution, and (3) visualization or post-processing, as seen in Fig. 2.

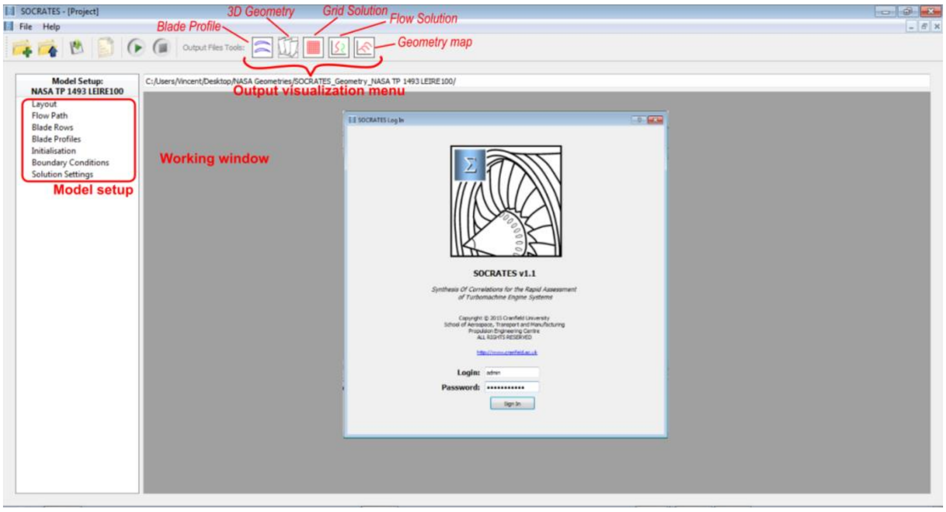

Figure 2 SOCRATES GUI main window workspace.

In general, the model setup is related to the input files, the solution to the program execution, and the post-processing to the output files. Fig. 3 displays a general structure diagram of the GUI, where the different processes for the model setup and post-processing are laid out.

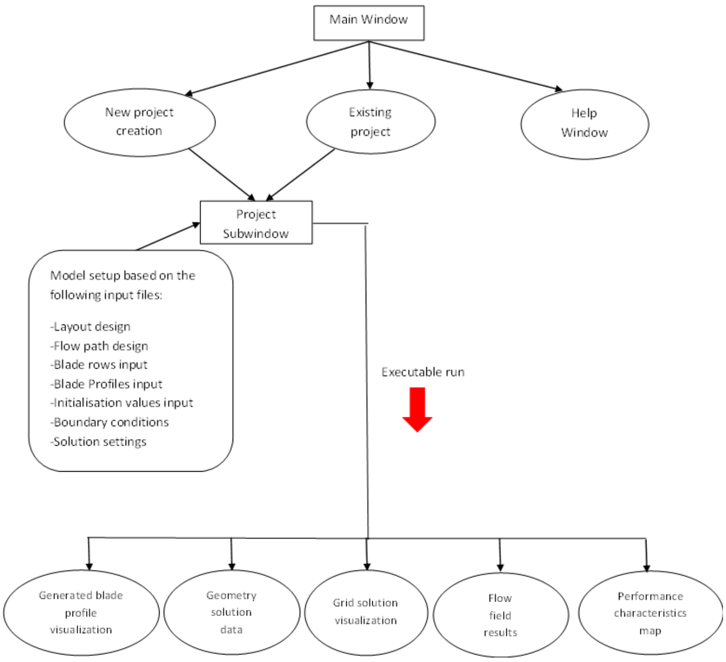

Figure 3 SOCRATES GUI structure for model setup and post-processing.

2.2.1 Model Setup

The first step to characterize the compressor or fan model is to define the number of stages (rotor, stator), inlet guide vane (IGV), outlet guide vane (OGV), or swirler. Additional ducts can be added at the inlet or outlet to capture the flow field properties ahead or behind the active turbo-components as observed in Fig. 4.

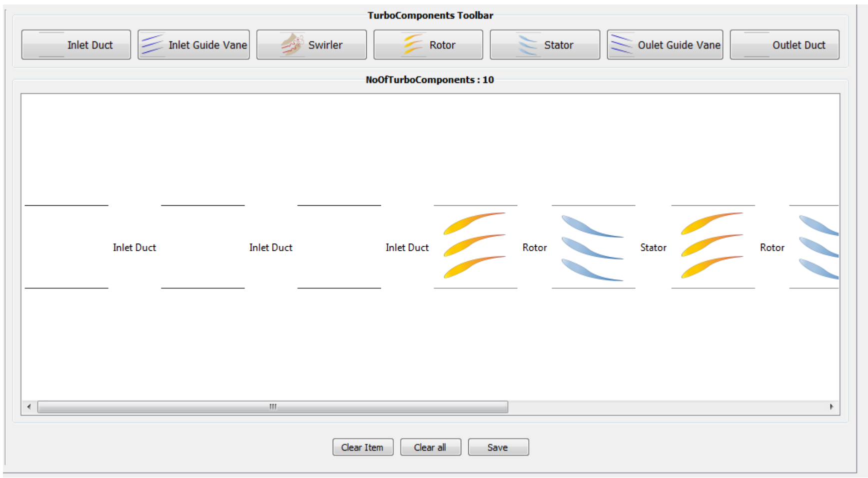

Figure 4 Compressor layout model to define the number and type of turbo-components.

The compressor flow path is defined through non-dimensional x and z Cartesian coordinates that allow a potential compressor scaling, based on a maximum flow path length and maximum radius, as illustrated in Fig. 5.

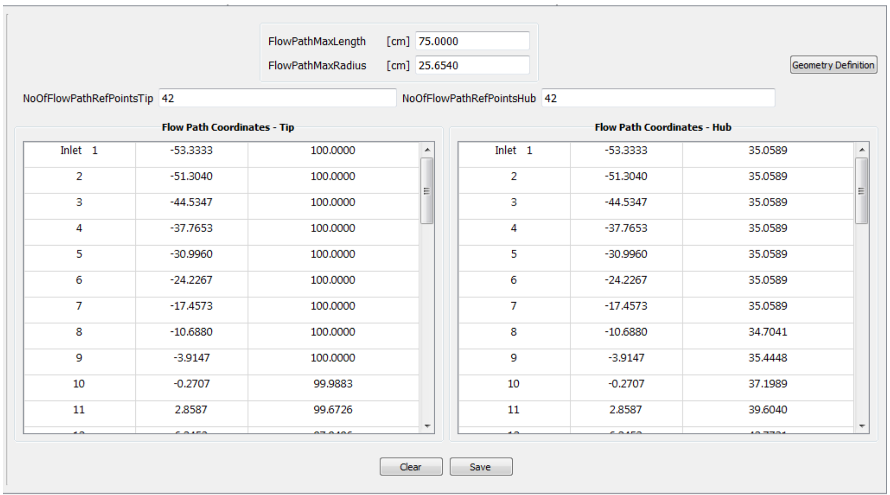

Tip			Hub		
Inlet 1	-53.3333	100.0000	Inlet 1	-53.3333	35.0589
2	-51.3040	100.0000	2	-51.3040	35.0589
3	-44.5347	100.0000	3	-44.5347	35.0589
4	-37.7653	100.0000	4	-37.7653	35.0589
5	-30.9960	100.0000	5	-30.9960	35.0589
6	-24.2267	100.0000	6	-24.2267	35.0589
7	-17.4573	100.0000	7	-17.4573	35.0589
8	-10.6880	100.0000	8	-10.6880	34.7041
9	-3.9147	100.0000	9	-3.9147	35.4448
10	-0.2707	99.9883	10	-0.2707	37.1989
11	2.8587	99.6726	11	2.8587	39.6040

Figure 5 Non-dimensional flow path coordinates definition.

The turbo-component blade row points are specified through non-dimensional x and z Cartesian coordinates. For the case of the rotors and stator, additional information is required, such as number of blades, clearance, and the design performance parameters used for the empirical loss and deviation models, as displayed in Fig. 6.

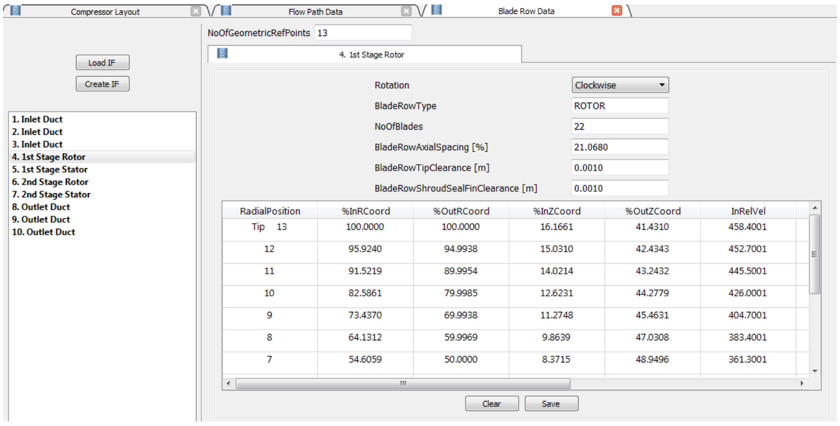

Figure 6 Turbo-component blade row definition using non-dimensional coordinates.

To define the blade profiles, blade elements are specified by radial section, which are laid out according to a constant surface turning on a conical surface [43] and stacked along their centre-of-area. Fig. 7 shows the blade-element definition in the SOCRATES GUI.

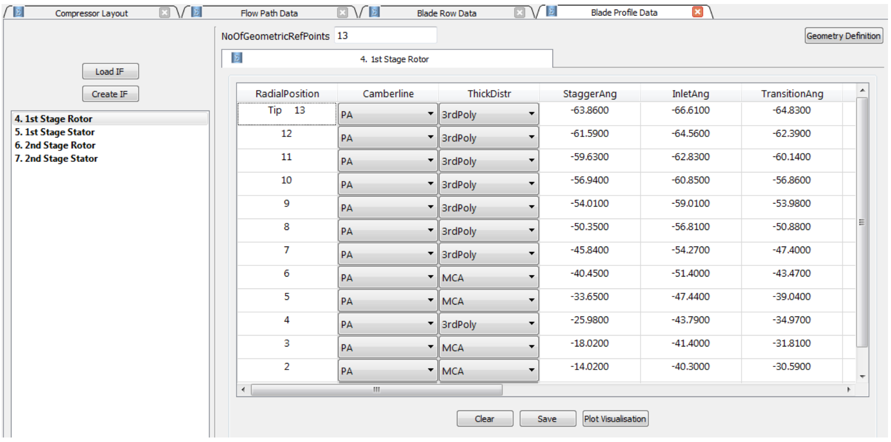

Figure 7 Blade-profile-element definition for different radial positions.

Because the solution of the REE is an interative approach, initialization values for the mean-line meridional velocities at the turbo-component inlets and outlets are specified. Additionally, endwall blockage factors can be indicated at the blade row inlets and outlets. Mean-line meridional velocities and blockage factors are given as in Fig. 8.

Figure 8 Initialization values and blockage factors specification.

In terms of the design and off-design cases to analyse, different speedline points can be specified where particular boundary conditions can be established for them as depicted in Fig. 9. As mentioned in Sec. 1, either inlet mass flow or outlet static pressure can be used as boundary condition.

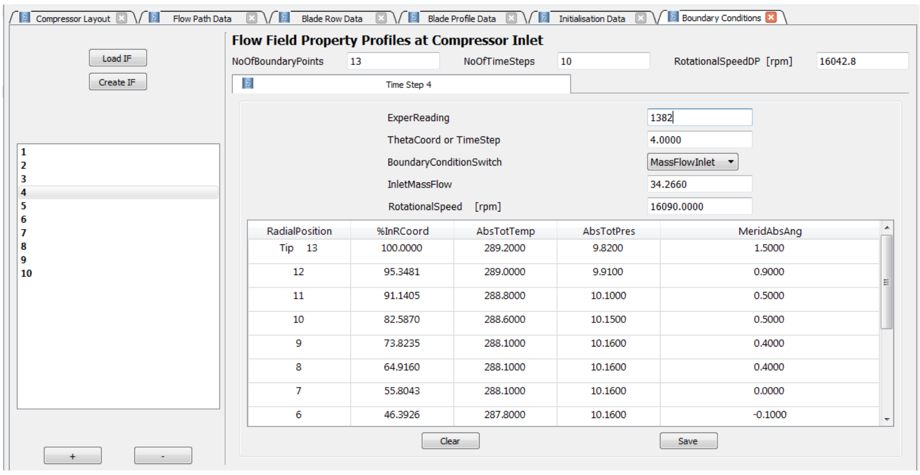

Figure 9 Boundary conditions for every speedline operating point specified.

To finalize the model setup, solution settings are specified in terms of the number of streamlines for the grid, damping factor for streamline radius movement between iterations, and the different error tolerances to satisfy boundary conditions.

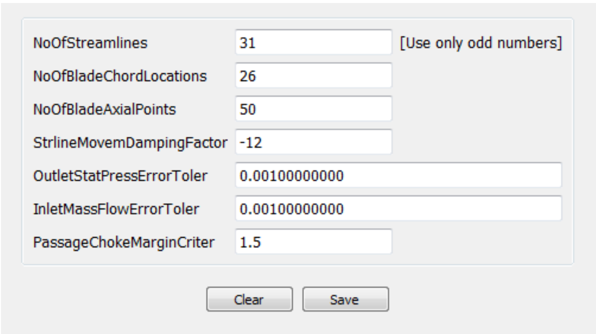

Figure 10 Solution settings input.

2.2.2 Solution

The SOCRATES execution can be performed directly in the GUI or through a quick launching tool developed that allows a selection of the different compressor/fan geometries available. The quick launcher allows GUI access in case a model is modified or a new compressor is defined.

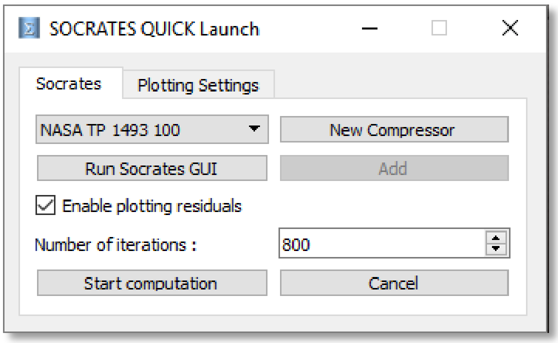

Figure 11 Quick launcher to directly run SOCRATES or start the GUI.

A vast library or compressor and fan geometries have been modelled over the development years of SOCRATES. Currently, the following geometries are available in SOCRATES: NASA Two Stage Fan [44], NASA Rotor 67 [45], NASA Rotor 66 [46], NASA Rotor 37 [47], NASA ADP Fan [48], NASA QF-1 Fan [49] [50], NASA Compressor 74A [51], NASA Two-Stage Fan with Dampers[52] and the NASA Stage

38 [53]. In this paper, the NASA Two-Stage Fan [44] is used as instance to display the different GUI utilities.

During running time, the residuals for the steamtube inlet and outlet mass flow errors for each turbo-component are plotted to track convergence. Fig. 12 shows the residuals graphs, which are constantly updated at every iteration.

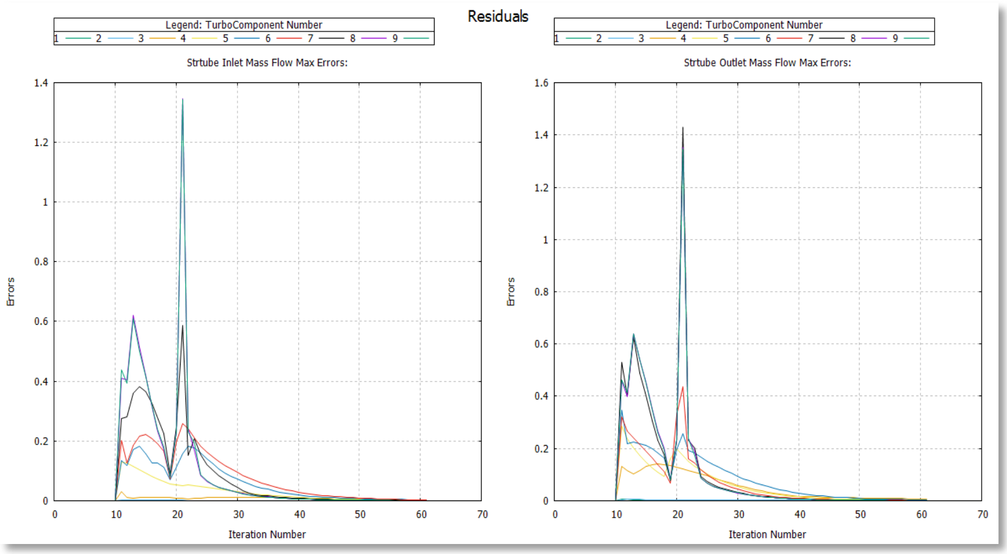

Figure 12 Iteration residuals plots for the inlet and oulet of each turbo-component.

Once the computation converges, output files for geometry, flow field parameters and performance characteristics are generated.

2.2.3 Visualization

The compressor flowpath sketch is visualized in a 2-D meridional plane, where the defined turbo-components are laid out as seen in Fig. 13.

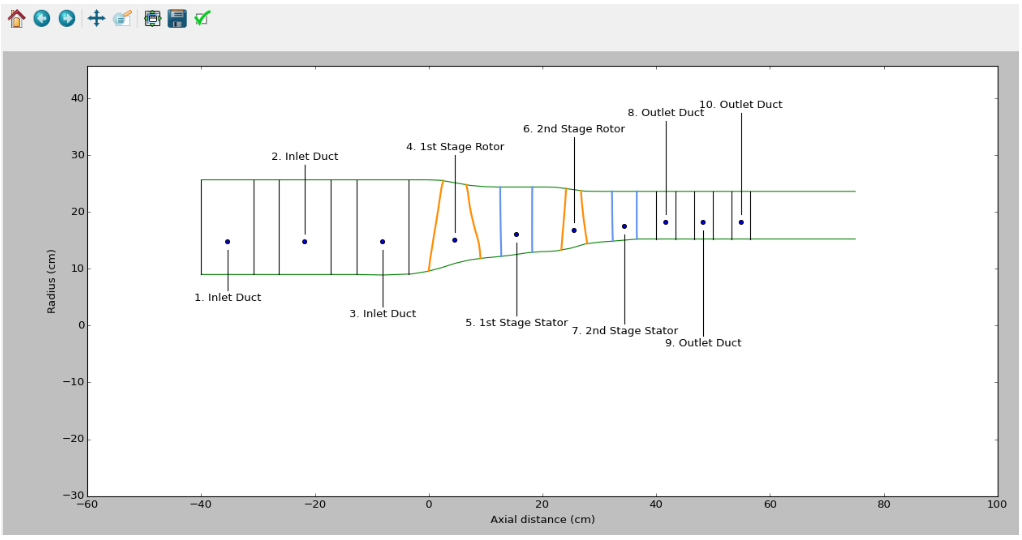

Figure 13 Axial-flow compressor 2-D view in the meridional plane.

Similarly, a blade-to-blade view can be obtained for every blade radial position assigned to appreciate the profile, as observed in Fig. 14. Further, a tabulation for the blade profile Cartesian coordinates in the x, y and z –axis is provided.

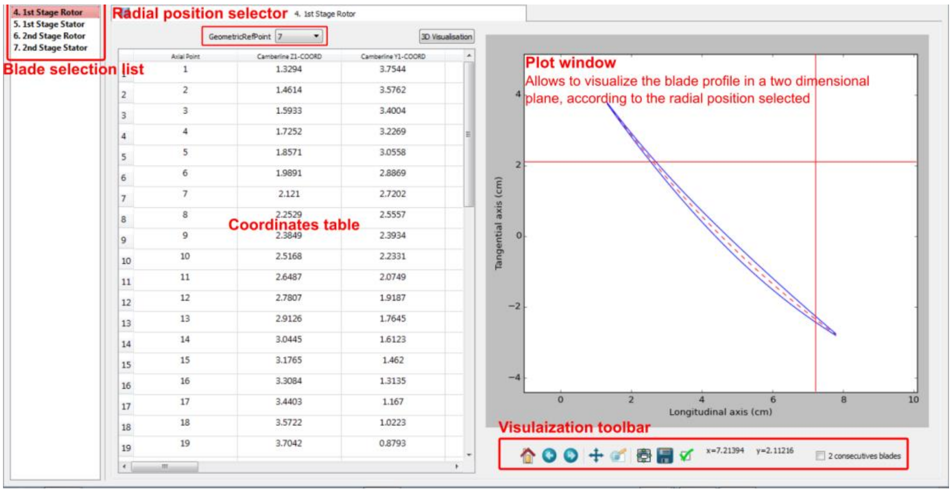

Figure 14 Blade-profile-section 2-D view in the blade-to-blade plane.

Due to the blade-element layout method implemented, full 3-D coordinates are obtained for the whole compressor/fan geometry. The 3-D view of the compressor flowpath and blading can be visualized as depicted in Fig. 15.

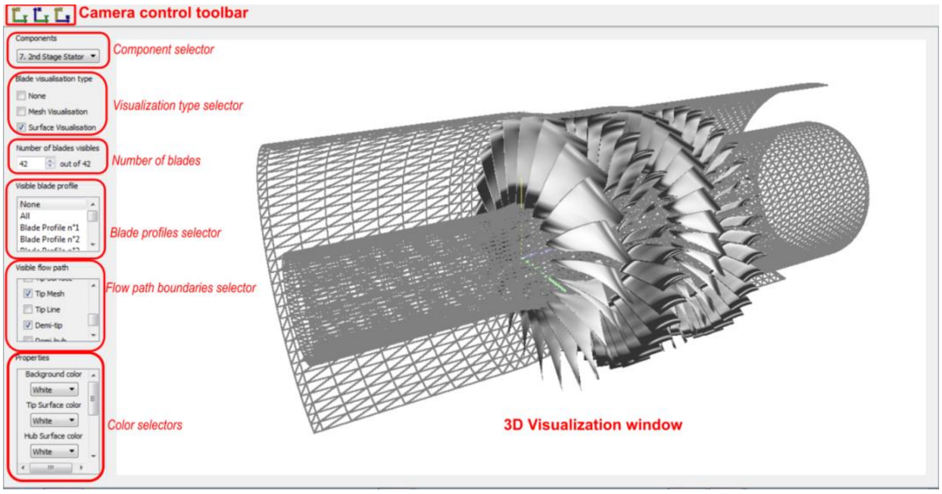

Figure 15 3-D visualization for the NASA two-stage fan [44].

The final mesh established between the converged streamlines and their corresponding quasi-orthogonals can be visualized as in Fig. 16. A more detailed zoom into the grid allows identifying the streamline displacement at the endwalls due to the blockage factors as shown in Fig. 17.

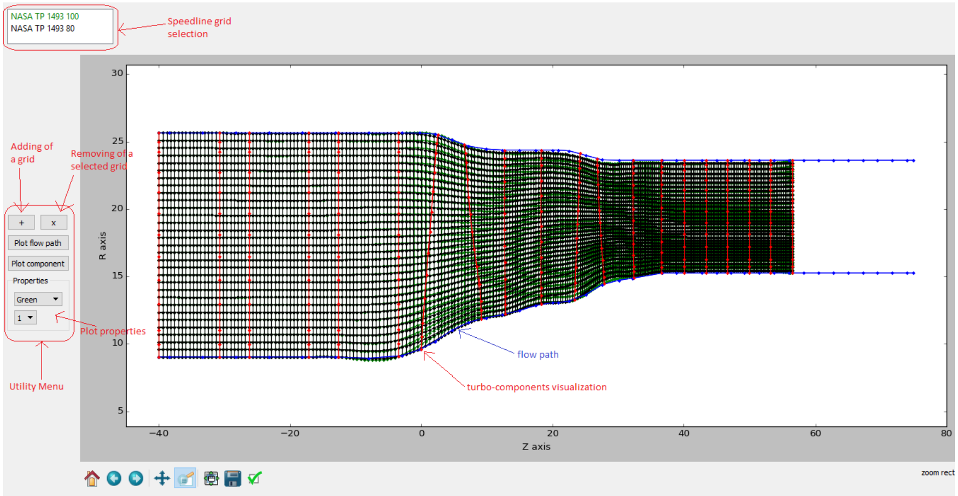

Figure 16 2-D final grid in the meridional plane composed by converged streamlines and quasi-orthogonals.

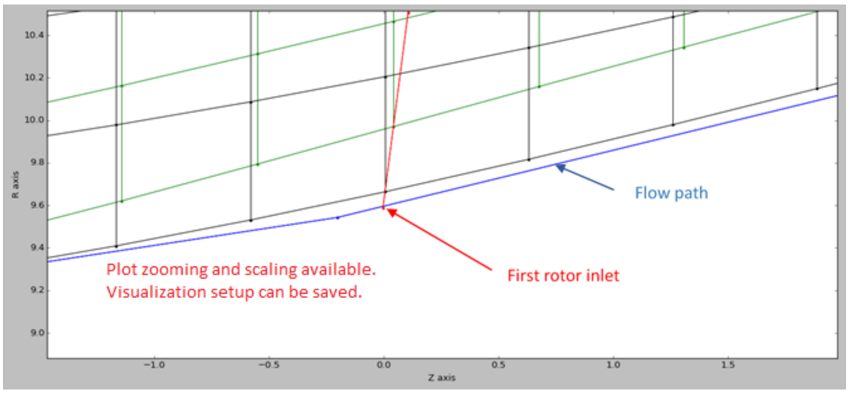

Figure 17 Computaional 2-D grid visualization zoom at hub endwall.

3.0 RESULTS

To show the SOCRATES GUI results post-processing, the NASA Two-Stage Fan [44] was modelled, simulated and used to illustrate this section. Table 1 lists the design overall parameters for this two-stage fan.

Table 1 NASA Two-Stage Fan [44] design overall parameters

Parameter	
Rotational Speed [rpm]	160428.8000
Fan Total Pressure Ratio	2.3990
Fan Total Temperature Ratio	1.3340
Fan Adiabatic Efficiency	0.8490
Mass Flow [kg/s]	33.2480
First-Stage Tip Speed [m/s]	428.8960

3.1 Flow Field Parameters

A post-processing plotting tool was developed to plot the flow field properties at each turbo-component blade row station. For direct response comparison between the same or different turbo-component inlet and outlet blade rows, several curves can be plotted in the same graph as seen in Fig. 18. Typically, spanwise properties distribution is desired; however, the post-processing tool allows modifying the variables in both graph axes.

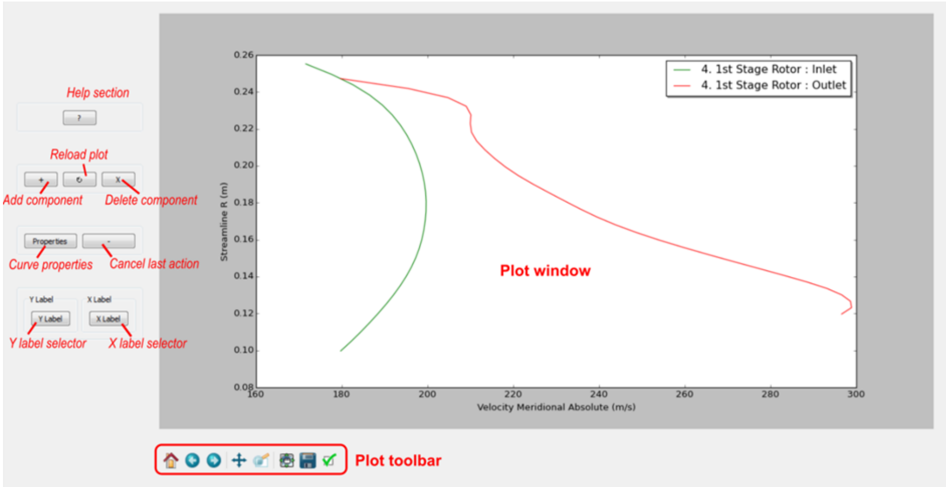

Figure 18 Flow field properties plotting

Fig. 19 shows the potential of the tool to compare different properties. In this case, the 1st stage rotor inlet against the outlet behaviour at $w = 34.515\ kg/s$ and design speed is compared.

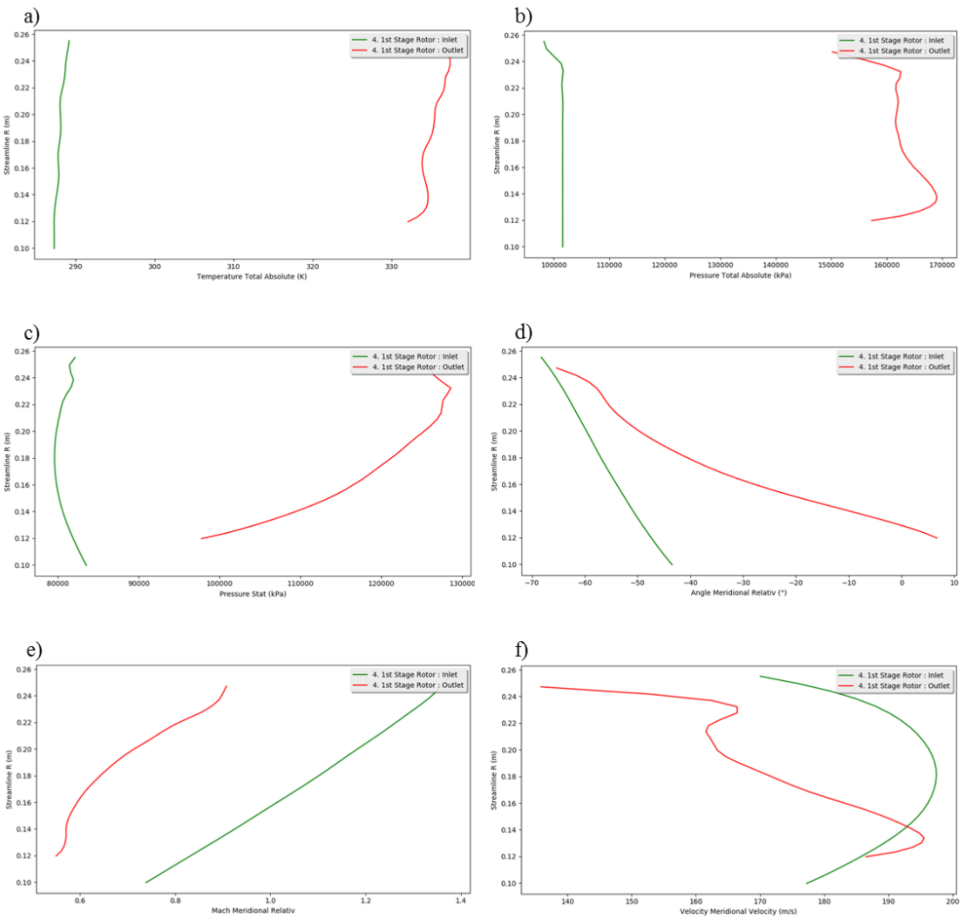

Figure 19 2-D SLC NASA Two-Stage Fan [44] flow field parameters for the 1st stage rotor inlet and outlet. a) Absolute total temperature b) Absolute total pressure c) Static pressure d) Relative meridional flow angle e) Relative Meridional Mach number f) Meridional Velocity

Apart from flow field parameters, blade-profile elements can also be plotted at every streamline radial location. Fig. 20 displays the aero-chord spanwise distribution.

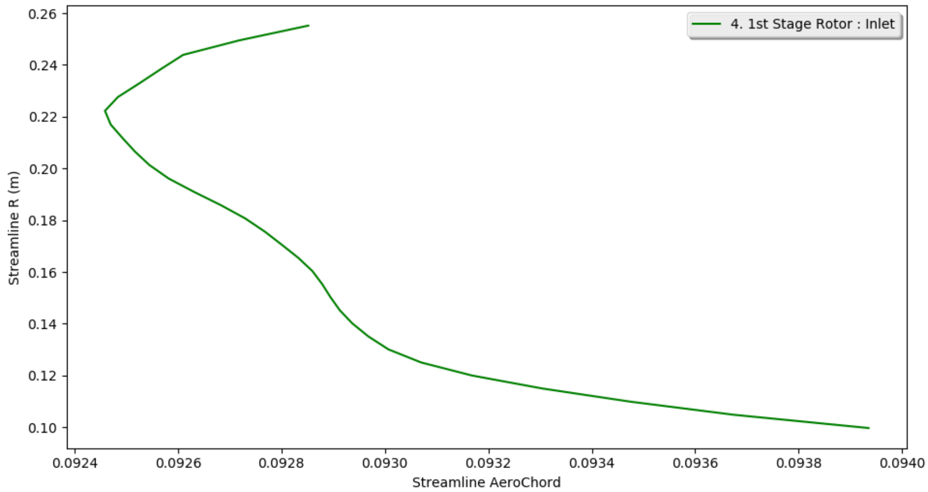

Figure 20 NASA Two-Stage Fan [44] 1st stage rotor blade aero-chord

To validate the 2-D SLC flow field from the GUI, Fig. 21 shows a comparison against measured data, where consistent agreement is obtained and no significant differences are observed.

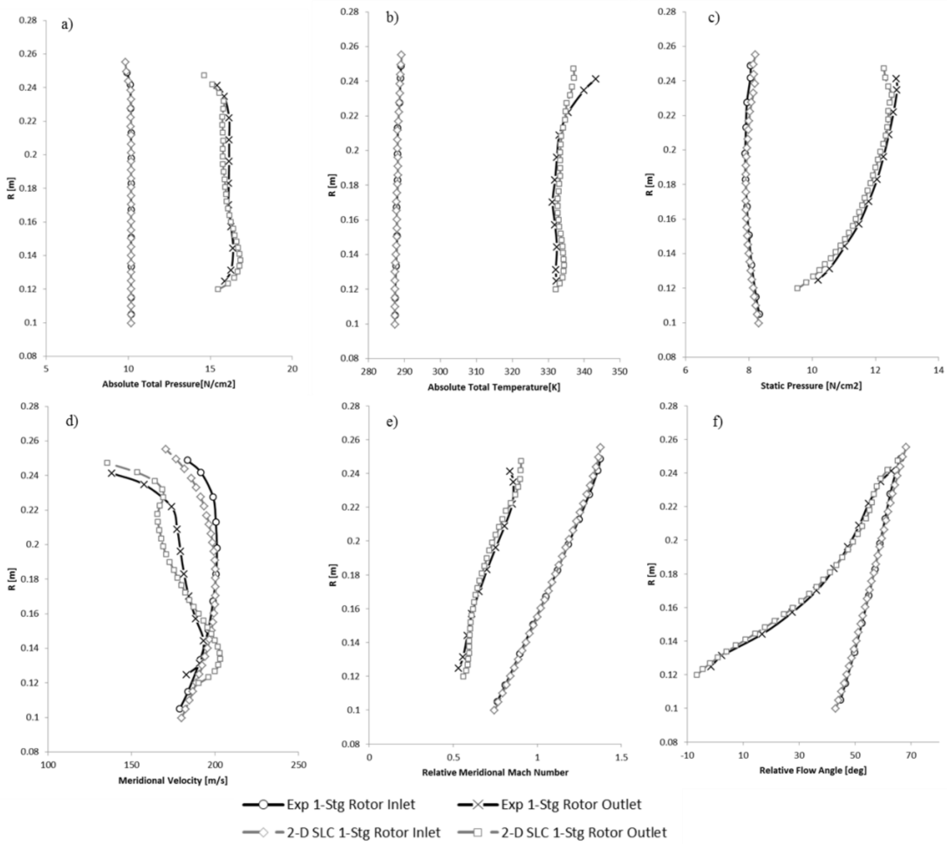

Figure 21 NASA Two-Stage Fan [44] flow field parameters comparison between experimental data and 2-D SLC for the 1st stage rotor inlet and outlet. a) Absolute total temperature b) Absolute total pressure c) Static pressure d) Relative meridional flow angle e) Relative Meridional Mach number f) Meridional Velocity

3.2 Performance Characteristics

A different workspace is used by the post-processing tool to plot the performance map for different speedlines analysed. The number of operating points appearing on the map depends on the number of cases specified in the boundary conditions. Fig. 22 shows the pressure ratio fan map for the NASA Two-Stage Fan, whereas in Fig. 23, the isentropic efficiency fan map is shown.

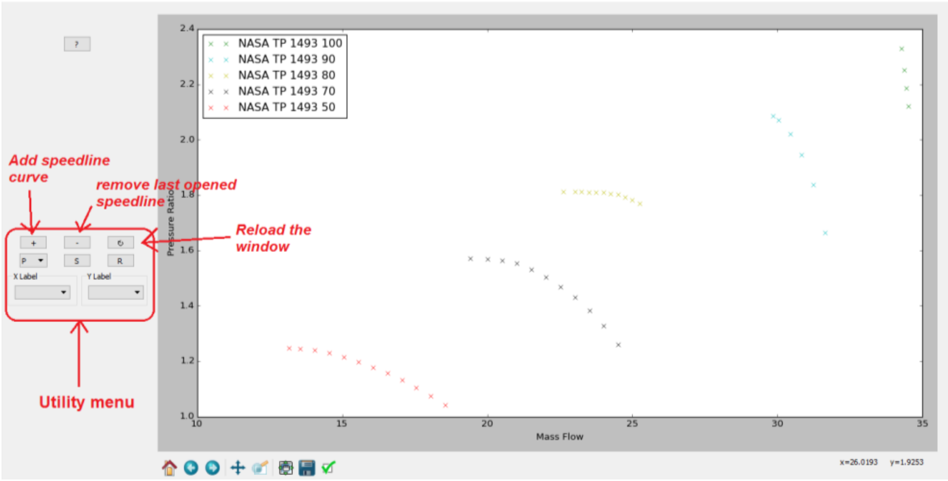

Figure 22 Fan pressure ratio map for the NASA two-stage fan [44] at 100, 90, 80, 70 and 50% of design speed.

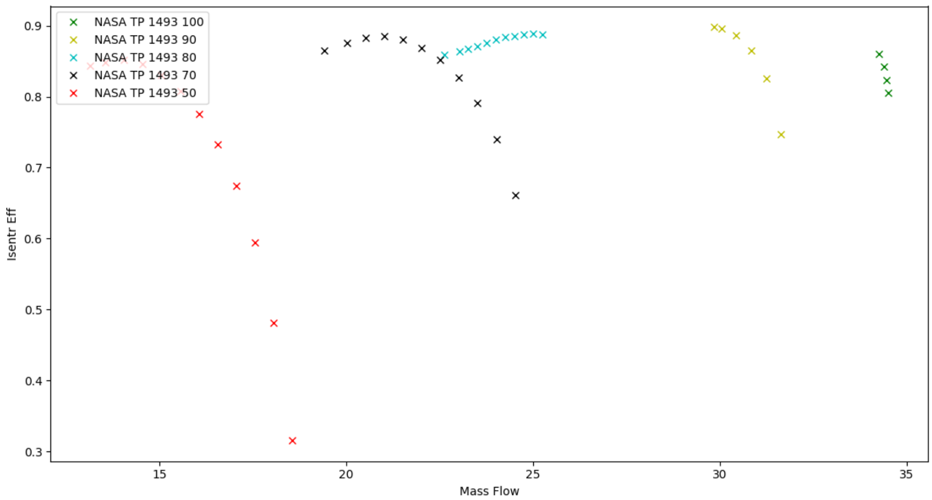

Figure 23 Fan isentropic efficiency map for the NASA two-stage fan [44] at 100, 90, 80, 70 and 50% of design speed.

The plotted 2-D SLC performance characteristics are compared against measured results in Fig. 24 for the pressure ratio and Fig. 25 for the isentropic efficiency. A satisfactory agreement is obtained for the pressure ratio. For the isentropic efficiency, although there is a difference between the experimental and simulated curves, there is a qualitative trend agreement. Difference in isentropic efficiency is less than 5% between the experimental and 2-D SLC data at the peak-efficiency points of each speedline. The difference is explained due to the empirical profile-loss models, which can be further fine-tuned to match the efficiency.

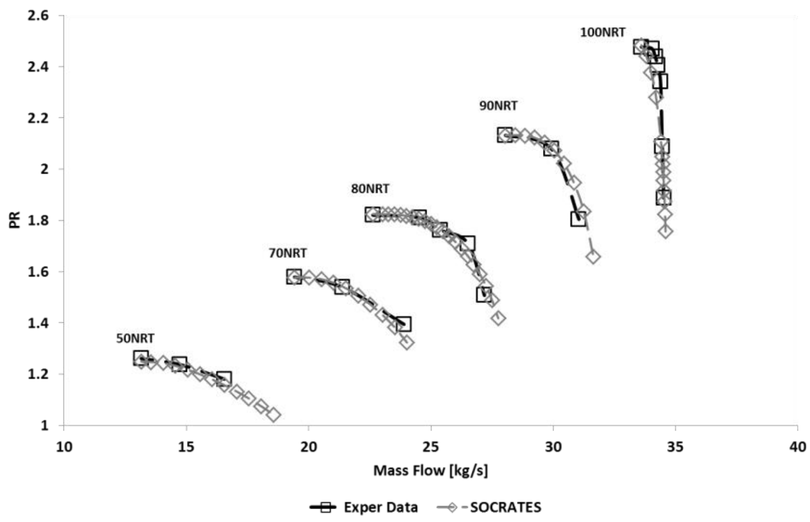

Figure 24 NASA Two-Stage Fan [44] pressure ratio map comparison between measured and 2-D SLC data.

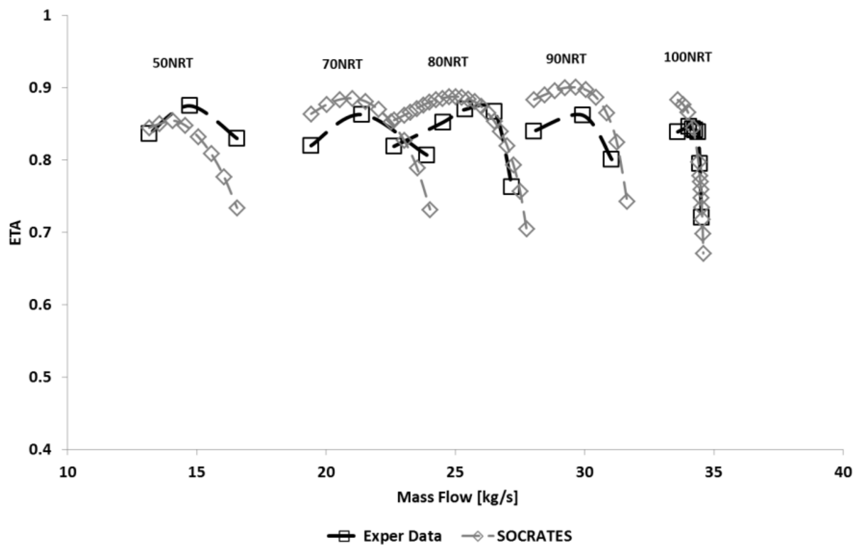

Figure 25 NASA Two-Stage Fan [44] isentropic efficiency map comparison between measured and 2-D SLC data.

4.0 CONCLUSIONS

The demand for more robust and accurate turbomachinery flow simulation methods and tools has expanded in the recent years. Unlike 3-D CFD analyses, 2-D SLC methods offer an acceptable solution in minutes. Because of the lack of open-source turbomachinery codes and the learning curve that user needs to go through, a GUI was developed for SOCRATES, an existing in-house 2-D SLC axial-flow compressor simulator. A GUI in this context helps to understand the 2-D SLC method itself and the axial-flow compressor aerodynamics, apart from saving time in the model preparation and results post-processing.

The SOCRATES GUI was built in three main sections: model setup, solution and visualization. The model setup handles the input files to define the compressor geometry, boundary conditions, initialization values, and solution settings. The solution module consists in a quick launcher to execute the simulation and mass flow residuals plotting during running time. In the visualization module, the axial-flow compressor is displayed in the 2-D meridional plane and in a 3-D view, along with a blade-to-blade projection for every blade-profile section. Furthermore, the visualization allows to post-process the result output files for the flow field properties at every turbo-component inlet and outlet, and for the compressor/fan performance map. Over the development years of SOCRATES, several axial-flow compressor geometries have been modelled. Among these, a NASA two-stage fan was used to validate the results obtained from GUI the post-processing. 2-D SLC flow field parameters and overall pressure ratio proved to be matched against experimental results. In terms of the isentropic efficiency map, differences less than 5% at the speedline peak-efficiencies were observed induced by the empirical loss models, nonetheless, the trend between 2-D SLC and measured data was consistent.

REFERENCES

1. Denton JD., Dawes WN. Computational Fluid Dynamics for Turbomachinery Design. Proceedings IMechE Part C: J. Mechanical Engineering Science. 1998; 213(2): 107–124.

2. Howell AR. Fluid dynamics of axial compressors. Proceedings of the IMechE. 1945; 153(1): 441–452.

3. Wu CH., Wolfenstein L. Application of radial-equilibrium condition to axial-flow compressor and turbine design. NACA Report. Lewis Flight Propulsion Laboratory, Cleveland, Ohio, United States of America: NACA Report 955; 1949. pp. 1–31.

4. Wright LC., Kovach K. Design Procedure and Limited Test Results for a High Solidity, 12-inch Transonic Impeller with Axial Discharge. NACA Research Memorandum. Lewis Flight Propulsion Laboratory, Cleveland, Ohio, United States of America: NACA RM E53B09; 1953. pp. 1–37.

5. Wright LC., Novak RA. Aerodynamic Design and Development of the General Electric CJ805-23 Aft-Fan. ASME Conference Proceedings. ASME Paper 60-WA-270; 1960.

6. Swan WC. A Practical Method of Predicting Transonic-Compressor Performance. Trans. ASME J. Power. 1961; 83(3): 322–330.

7. Smith Jr. LH. The Radial-Equilibrium Equation of Turbomachinery. Trans. ASME J. Engineering for Power. 1966; 88(1): 1–12.

8. Silvester MD., Hetherington R. A numerical solution of the three-dimensional compressible flow through axial turbomachinery in numerical analysis. Numerical Analysis - an Introduction. Oxford Academic Press; 1966.

9. Frost GR., Hearsey RM., Wennerstrom AJ. A Computer Program for the Specification of Axial Compressor Airfoils. ARL Report. Aerospace Research Laboratories, Air Force Systems Command, Wright-Patterson Air Force Base, Dayton, Ohio, United States of America: ARL 72-0171; NTIS AD-785 879; 1972. pp. 1–158.

10. Pachidis V. Gas Turbine Advanced Performance Simulation. PhD Thesis. Cranfield University, School of Engineering, Cranfield, United Kingdom; 2006. pp. 1–384.

11. Novak RA. Streamline Curvature Computing Procedures for Fluid-Flow Problems. Trans. ASME J. Engineering for Gas Turbines and Power. 1967; 89(4): 478–490.

12. Wu CH. A General Through Flow Theory of Fluid Flow with Subsonic or Supersonic Velocity in Turbomachines Having Arbitrary Hubs and Casing Shapes. NASA Technical Note. NASA TN 2388; 1951.

13. Denton JD. Some Limitations of Turbomachinery CFD. ASME Turbo Expo 2010: Power for Land, Sea and Air. 14-18 June, Glasglow, United Kingdom: GT2010-22540; 2010. pp. 1–11.

14. Pachidis V., Pilidis P., Marinai L., Templalexis I. Towards a Full Two Dimensional Gas Turbine Performance Simulator. Aeronautical J. 2007; 111(1121): 433–442.

15. Pachidis V., Pilidis P., Templalexis I., Alexander T., Kotsiopoulos P. Prediction of Engine Performance Under Compressor Inlet Flow Distortion Using Streamline Curvature. ASME Turbo Expo 2006: Power for Land, Sea and Air. 8-11 May, Barcelona, Spain: GT2006-90806; 2006. pp. 1–17.

16. Pachidis V., Pilidis P., Templalexis I., Korakianitis T., Kotsiopoulos P. Prediction of Engine Performance Under Compressor Inlet Flow Distortion Using Streamline Curvature. ASME J. Engineering for Gas Turbines and Power. 2007; 129(1): 97–103.

17. Tiwari P., Stein A., Lin Y-L. Dual-Solution and Choked Flow Treatment in a Streamline Curvature Throughflow Solver. ASME J. Turbomachinery. 2013; 135(4): 1–11.

18. Templalexis I., Pilidis P., Pachidis V., Kotsiopoulos P. Development of a Two-Dimensional Streamline Curvature Code. ASME J. Turbomachinery. 2011; 133(1): 1–7.

19. Boyer KM. An Improved Streamline Curvature Approach for Off-Design Analysis of Transonic Axial Compression Systems. PhD Thesis. Virginia Polythenic Institute and State University, Blacksburg, Virginia, United States of America; 2001. pp. 1–168.

20. Sayari N., Bolcs A. A New Throughflow Approach For Transonic Axial Compressor Stage Analysis. ASME 1995 Int. Gas Turbine and Aeroengine Congress and Exposition. 5-8 June, Houston, Texas, United States of America: 95-GT-195; 1995. pp. 1–12.

21. Creveling HF., Carmody RH. Axial Flow Compressor Computer Program for Calculating Off-Design Performance (Program IV). NASA Contract Report. Lewis Research Center, Cleveland, Ohio, United States of AmERICA: CR-72427; EDR-5898; 1968. pp. 1–258.

22. Hearsey RM. A computer Program for Axial Compressor design, Vol. 1: Theory Descriptions, and users Instructions. Technical Report. Dayton University, Cincinnati, Ohio, United States of America: AFAPL-TR-73-66-VOL-1; 1973.

23. Hearsey RM. A Computer Program for Axial Compressor Design, Vol. 1: Theory Descriptions, and User Instructions. Technical Report. Dayton University, Cincinnati, Ohio, United States of America: AD-A 009273; 1975.

24. Glenny DE. An Application of Streamline Curvature Methods to the Calculations of Flow in a Multistage Axial Compressor. Mechanical Engineering Note. Australian Defense Scientific Service, Aeronautical Research Laboratories: ARL/ME 346; 1974.

25. Denton JD. Through-flow calculations for transonic axial flow turbines. Trans. ASME J. Engineering for Power. 1978; 100(2): 212–218.

26. Jennions IK., Stow P. The Quasi-Three-Dimensional Turbomachinery Blade Design System, Part I: Through-Flow Analysis. Trans. ASME J. Engineering for Gas Turbines and Power. 1985; 107(2): 308–314.

27. Barbosa JR. A Streamline Curvature Computational Programme for Axial Compressor Performance Prediction. PhD Thesis. Cranfield Institute of

Technology, School of Mechanical Engineering, Cranfield, United Kingdom; 1987. pp. 1–183.

28. Ucer AS., Shreeve RP. A Viscous Axisymmetric Throughflow Prediction Method for Multi-Stage Compressors. ASME Int. Gas Turbine & Aeroengine Congress & Exposition. 1-4 June, Cologne, Germany: 92-GT-293; 1992. pp. 1–11.

29. Zhu XC., Hu JF., Ou-Yang H., Tian J., Qiang XQ., Du ZH. The Off-Design Performance Prediction of Axial Compressor Based on a 2D Approach. J. Theoretical and Applied Mechanics. 2013; 51(3): 523–531.

30. Turner MG., Merchant A., Bruna D. A Turbomachinery Design Tool for Teaching Design Concepts for Axial-Flow Fans, Compressors, and Turbines. ASME J. Turbomachinery. 2011; 133(3): 1–12.

31. Genrup M., Carlsson I., Engdar U., Assadi M. A Reduced-Order Through-Flow Program for Choked and Cooled Axial Turbines. ASME Turbo Expo 2005: Int. Gas Turbine & Aeroengine Congress. 6-9 June, Reno, Nevada, United States of America: GT2005-68716; 2005. pp. 1161–1168.

32. Mattingly JD., Heiser WH., Pratt DT. Aircraft Engine Design. 2002.

33. Mattingly JD. Elements of Gas Turbine Propulsion. AIAA Education Series; 2005.

34. Templalexis I., Pilidis P., Pachidis V., Kotsiopoulos P. Development of a 2-D Compressor Streamline Curvature Code. ASME Turbo Expo 2006: Power for Land, Sea and Air. 8-11 May, Barcelona, Spain: GT2006-90867; 2006. pp. 1–10.

35. Templalexis I. The Importance of Force Terms Modeling Within the Streamline Curvature Through-Flow Method. Proceedings IMechE Part A: J. Power and Energy. 20 June 2014; 228(7): 825–835.

36. Lieblein S. Aerodynamic Design of Axial-Flow Compressors. NASA Special Publication. Washington, D.C., United States of America: NASA SP-36 Chapter VI; 1965. pp. 183–226.

37. Carter ADS. The Low Speed Performance of Related Aerofoils in Cascades. Aeronautical Research Council Current Papers. Ministry of Technology, London, United Kingdom: C. P. No. 55; 1949. pp. 1–20.

38. Lieblein S. Incidence and Deviation-Angle Correlations for Compressor Cascades. Trans. ASME J. of Basic Engineering. 1960; 82(3): 575–584.

39. Cetin M., Ucer AS., Hirsch C., Serovy GK. Application of Modified Loss and Deviation Correlations to Transonic Axial Compressors. NATO Advisory Group for Aerospace Research and Development Report. Neuilly sur Seine, France: AGARD-R-745; 1987. pp. 1–74.

40. Aungier RH. Axial-Flow Compressors. 1st edn. New York, New Yor, United States of America: ASME Press; 2003. 368 p.

41. Cunnan WS., Stevans W., Urasek DC. Design and Performance of a 427-Meter-Per-Second-Tip-Speed Two-Stage Fan Tip-Speed Two-Stage Fan Having a 2.40 Pressure Ratio. NASA Technical Paper. Lewis Research Center, Cleveland, Ohio, United States of America: NASA TP-1314; 1978. pp. 1–94.

42. Pachidis V., Templalexis I., Pilidis P., Kotsiopoulos P. A Dynamic Convergence Control Scheme for the Solution of the Radial Equilibrium Equation in Through-flow Analyses. Proceedings IMechE Part G: J. Aerospace Engineering. 2009; 224(G7): 803–815.

43. Crouse JE., Junetzke DC., Schwirian RE. A Computer Program for Composing

Compressor Blading from Simulated Circular-Arc Elements on Conical Surfaces. NASA Technical Note. Lewis Research Center, Cleveland, Ohio, United States of America: NASA TN D-5437; 1969. pp. 1–82.

44. Urasek DC., Gorrell WT., Cunnan WS. Performance of Two-Stage Fan Having Low-Aspect Ratio, First-Stage Rotor Blading. NASA Technical Paper. Lewis Research Center, Cleveland, Ohio, United States of America: NASA TP-1493; AVRADCOM TR 78-49; 1979. pp. 1–131.

45. Strazisar AJ., Wood JR., Hathaway MD., Suder KL. Laser Anemometer Measurements in a Transonic Axial-Flow Fan Rotor. NASA Technical Paper. Lewis Research Center, Cleveland, Ohio, United States of America: NASA TP-2879; 1989. pp. 1–214.

46. Urasek DC., Steinke RJ., Lewis GW. Performance of Inlet Stage of Transonic Compressor. NASA Technical Memorandum. Lewis Research Center, Cleveland, Ohio, United States of America: NASA TM X-3345; 1976. pp. 1–71.

47. Moore RD., Reid L. Performance of Single-Stage Axial-Flow Transonic Compressor with Rotor and Stator Aspect Ratios of 1.63 and 1.77, Respectively, and with Design Pressure Ratio of 2.05. NASA Technical Paper. Lewis Research Center, Cleveland, Ohio, United States of America: NASA TP-1659; 1980. pp. 1–102.

48. Hobbs DE., Neubert RJ., Malmborg EW., Philbrick DH., Spear DA. Low Noise Research Fan Stage Design. NASA Contract Report. Lewis Research Center, Cleveland, Ohio, United States of America: NASA CR-195382; 1995. pp. 1–60.

49. Gelder TF., Soltis RF. Inlet Noise of 0.5-Meter-Diameter NASA QF-1 Fan as Measured in an Unmodified Compressor Aerodynamic Test Facility and in an Anechoic Chamber. NASA Technical Note. Lewis Research Center, Cleveland, Ohio, United States of America: NASA TN D-8121; 1975. pp. 1–97.

50. Gelder TF., Lewis Jr. GW. Aerodynamic Performance of 0.5-Meter-Diameter, 337-Meter-per-Second Tip Speed, 1.5-Pressure-Ratio, Single-Stage Fan Designed for Low Noise Aircraft Engines. NASA Technical Note. Lewis Research Center, Cleveland, Ohio, United States of America: NASA TN D-7836; 1974. pp. 1–182.

51. Steinke RJ. Design of 9.271-Pressure-Ratio Five-Stage Core Compressor and Overall Performance for First Three Stages. NASA Technical Paper. Lewis Research Center, Cleveland, Ohio, United States of America: NASA TP-2597; 1986. pp. 1–34.

52. Urasek DC., Cunnan WS., Stevans W. Performance of Two-Stage Fan with Larger Dampers on First-Stage Rotor. NASA Technical Paper. Lewis Research Center, Cleveland, Ohio, United States of America: NASA TP-1399; 1979. pp. 1–78.

53. Moore RD., Reid L. Performance of Single-Stage Axial-Flow Transonic Compressor with Rotor and Stator Aspect Ratios of 1.63 and 1.77, Respectively, and with Design Pressure Ratio of 2.05. NASA Technical Paper. Lewis Research Center, Cleveland, Ohio, United States of America: NASA TP-2001; 1982. pp. 1–115.